Promoting effect of nickel-chromium hydroxide on nickel phosphide nanosheets for efficient hydrogen production coupled with sulfion degradation

Xiaojun Wang,[a] Jieting Li,[a] Xinyu Zhu,[a] Zehua Xu,[a] Shuixiang Xie,[a] Shutong Chen, Yuxuan Wan,[a] Guangyu Zhang,[a] Mingzheng Ge,[a] Wei Zhang,[a] Chao Wang,*[,b] and Rui-Qing Li*[a]

Experimental section

Chemicals

Nickel foam (NF) was supplied by Taiyuan source of power company. Ethanol absolute (99.7 %) was purchased from Shanghai Lingfeng Chemical Reagent Co. Nickel (II) nitrate hexahydrate ($Ni(NO_3)_2{\cdot}6H_2O$), $CO(NH_2)_2$ were purchased from Sinopharm Chemical Reagent Co, Ammonium fluoride (H_4FN), Chromic acetate ($C_6H_9O_6Cr$) were purchased Shanghai Aladdin Biochemical Technology Co. Sodium hypophosphite (NaH_2PO_2) was purchased from Shanghai Macklin Biochemical Co.

Synthesis of $Ni_2P/NiCr(OH)_2$

The growth of $Ni_2P/NiCr(OH)_2$ on the NF surface was accomplished via a hydrothermal method followed by a phosphidation process. Initially, 2.0 mmol of $Ni(NO_3)_2$, 10.0 mmol of $CO(NH_2)_2$, and 6.0 mmol of NH_4F were dissolved in 35 mL of water and stirred to form a homogeneous solution. Subsequently, NF was immersed in the above solution and heated at 120 ℃ for 6 hours to obtain the $Ni(OH)_2$ precursor. Afterwards, a uniform solution was prepared by mixing 0.2 mmol of $C_6H_9O_6Cr$, 10.0 mmol of $CO(NH_2)_2$, 3.0 mmol of NH_4F, and 35 mL of water. The $Ni(OH)_2$ precursor was then transferred into this solution and heated at 150 ℃ for 6 hours to synthesize $NiCr(OH)_2$.Finally, the as-synthesized $NiCr(OH)_2$ was subjected to phosphidation with 0.1 g of NaH_2PO_2 at 400 ℃ for 2 hours under a high-purity nitrogen atmosphere.

For comparison, Ni_2P was also prepared under similar conditions, except that the phosphidation was carried out directly after the first hydrothermal step.

Materials characterization

The morphology and microstructure of $Ni_2P/NiCr(OH)_2$ were characterized by a GeminiSEM 300 field emission scanning electron microscope (FE-SEM) and a high-resolution transmission electron microscope (HRTEM), so as to clarify the dispersion state of the nanoparticles and the morphological characteristics of the fiber matrix. The crystal structure of $Ni_2P/NiCr(OH)_2$ was analyzed via X-ray diffraction (XRD) to confirm the phase composition of each component. X-ray photoelectron spectroscopy (XPS) was employed to determine the elemental composition and valence state distribution on the surface of the catalyst.

Electrochemical measurements

The electrochemical tests of the samples were performed on a Chenhua CHI660E electrochemical workstation in a standard three-electrode system. The as-prepared samples, graphite electrode, and Hg/HgO electrode served as the working electrode, counter electrode, and reference electrode, respectively. Linear sweep voltammetry (LSV) at a scan rate of 2 $mV \cdot s^{-1}$ was adopted to evaluate the catalytic activity of the samples; cyclic voltammetry (CV) was employed to calculate the double-layer capacitance (C_{dl}) of the $Ni_2P/NiCr(OH)_2$ electrodes; electrochemical impedance spectroscopy (EIS) was measured via electrochemical impedance spectroscopy in the frequency range of 0.1–10^5Hz; chronopotentiometry was used to record the voltage-time (v-t) curves for assessing the stability of the catalysts. The potentials obtained from the above electrochemical tests were converted to the reversible hydrogen electrode (RHE) scale using the Nernst equation: $E_{(RHE)}=E_{(Hg/HgO)}+0.0592\times pH+0.098$.

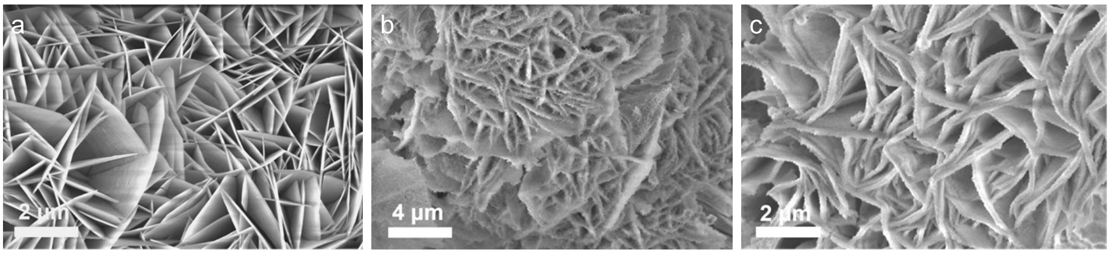

Fig. S1 SEM images of (b) $Ni(OH)_2$ (c)$Ni(OH)_2$/NiCr(OH) and (d) $Ni_2P/NiCr(OH)_2$

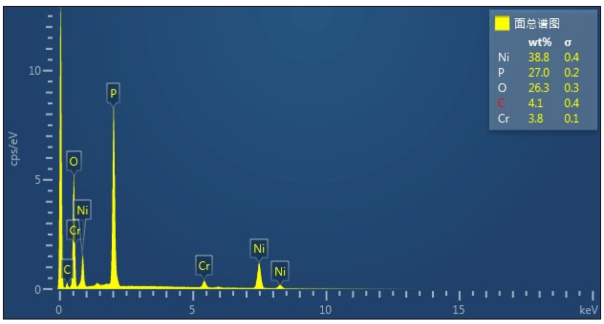

Fig. S2 The energy-dispersive X-ray spectrum of $Ni_2P/NiCr(OH)_2$.

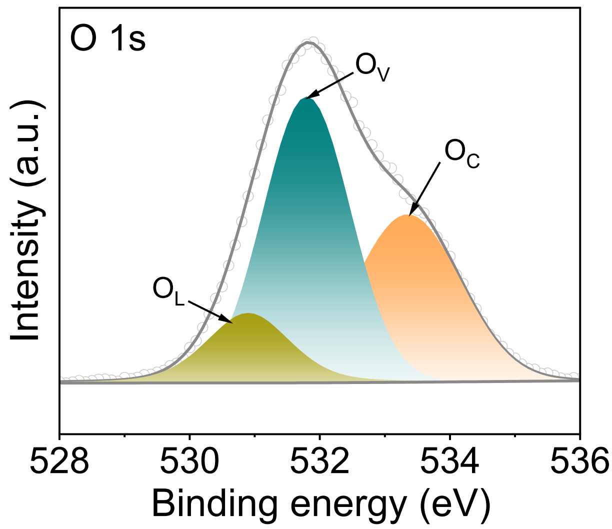

Fig. S3 O 1s XPS spectrum of $Ni_2P/NiCr(OH)_2$.

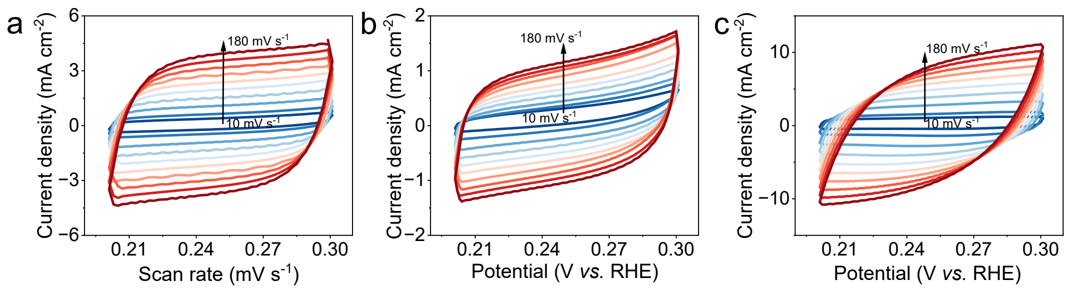

Fig. S4 CV curves at different sweep speeds of (a) $Ni_2P/NiCr(OH)_2$, (b)Ni_2P and (c) Pt/C.

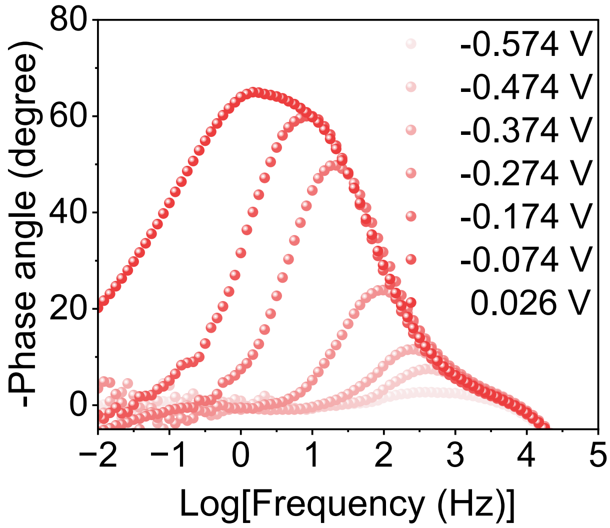

Fig. S5 Bode phase plots of Ni_2P toward HER.

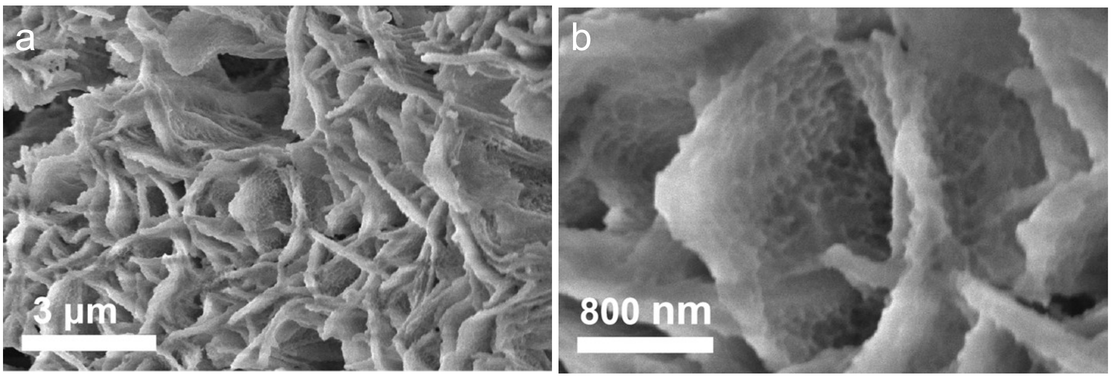

Fig. S6 SEM images of $Ni_2P/NiCr(OH)_2$ after the HER test.

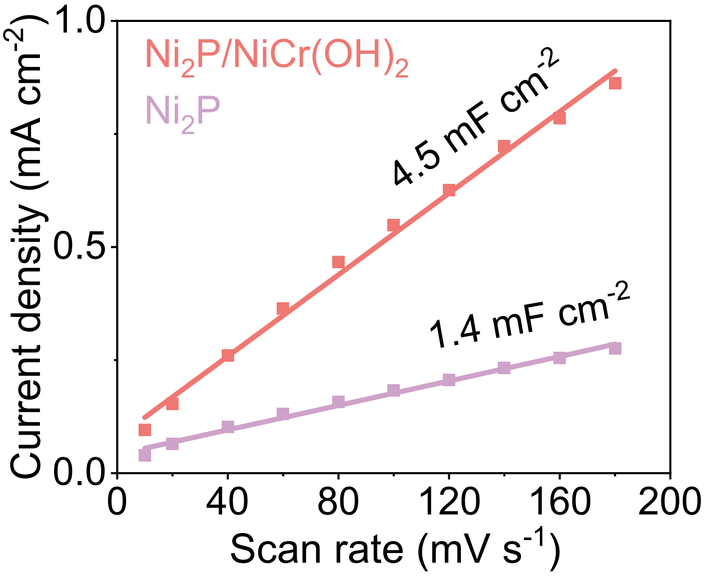

Fig. S7 C_{dl} values of different catalysts in 1 M KOH.

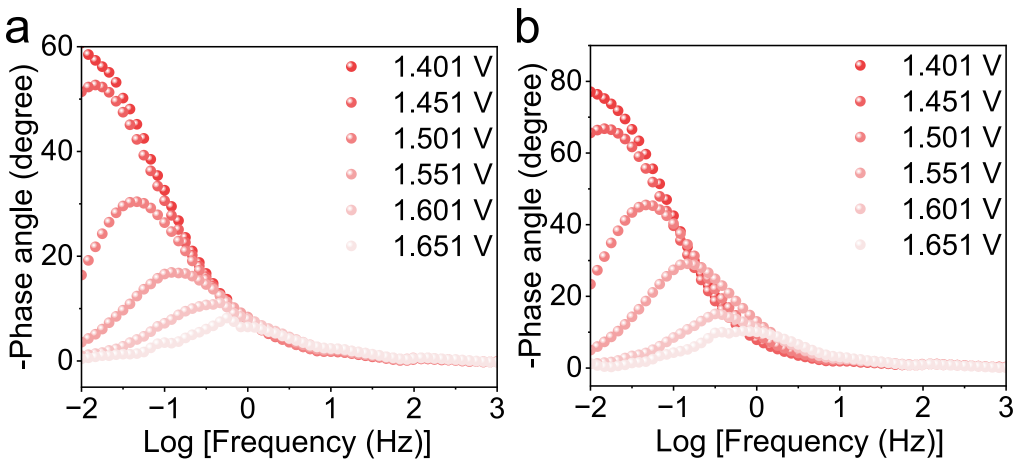

Fig. S8 Bode phase plots of (c) Ni_2P and (d) $Ni_2P/NiCr(OH)_2$ toward OER.

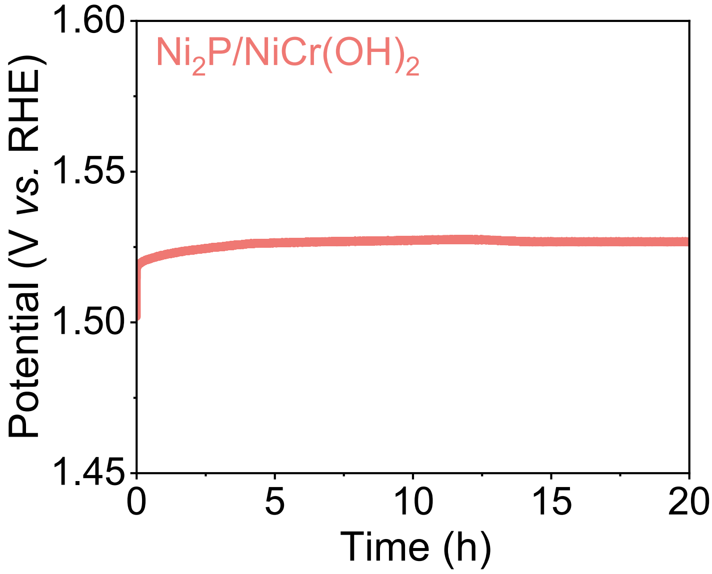

Fig. S9 Durability test of $Ni_2P/NiCr(OH)_2$ for OER.

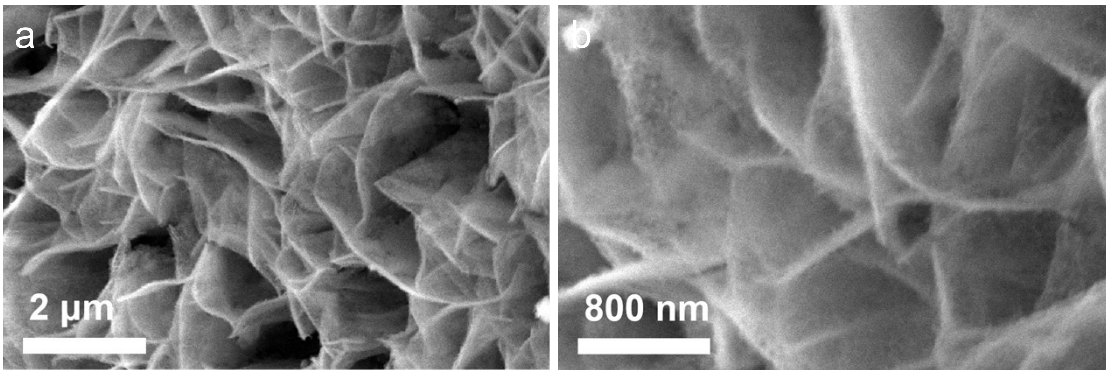

Fig. S10 SEM images of $Ni_2P/NiCr(OH)_2$ after the SOR test.

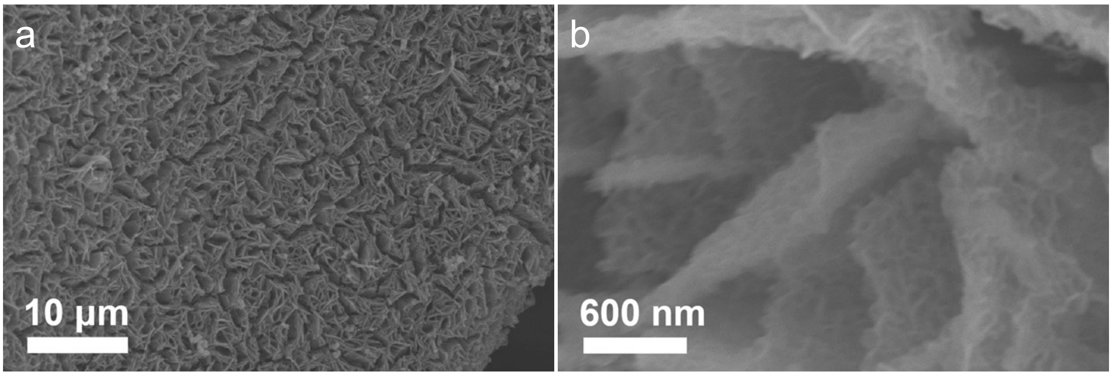

Fig. S11 SEM images of $Ni_2P/NiCr(OH)_2$ after the OER test.

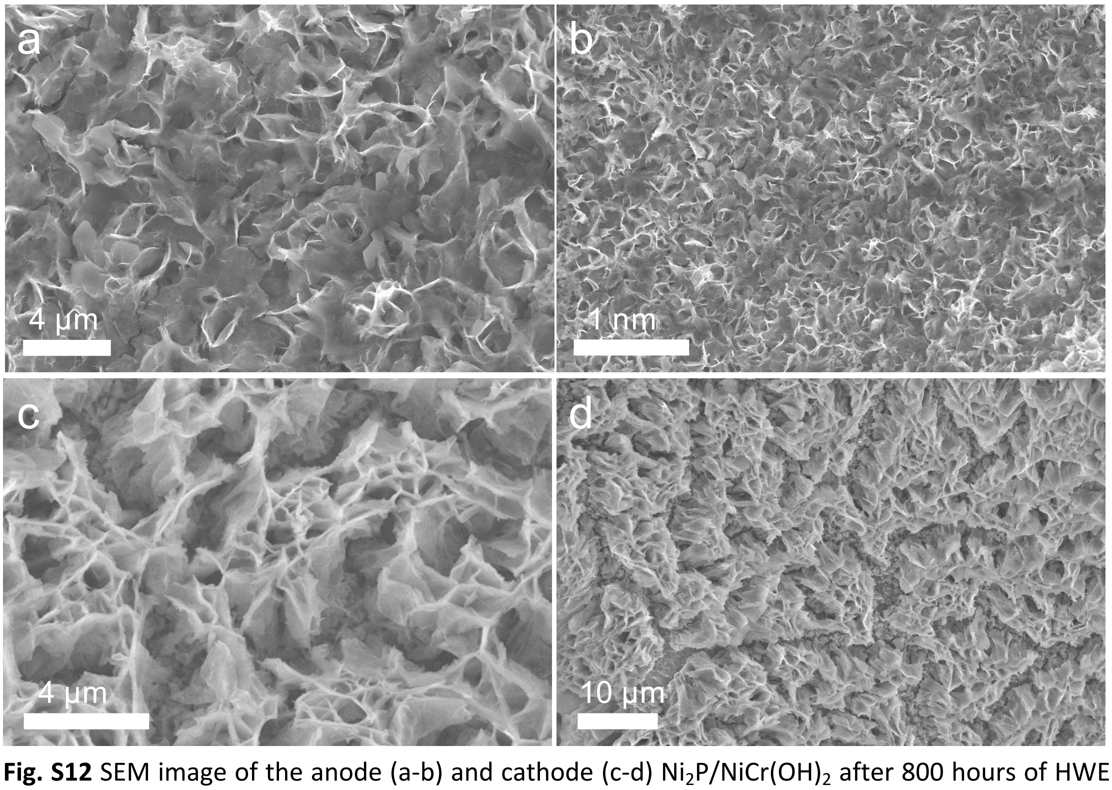

Fig. S12 SEM image of the anode (a-b) and cathode (c-d) $Ni_2P/NiCr(OH)_2$ after 800 hours of HWE testing.

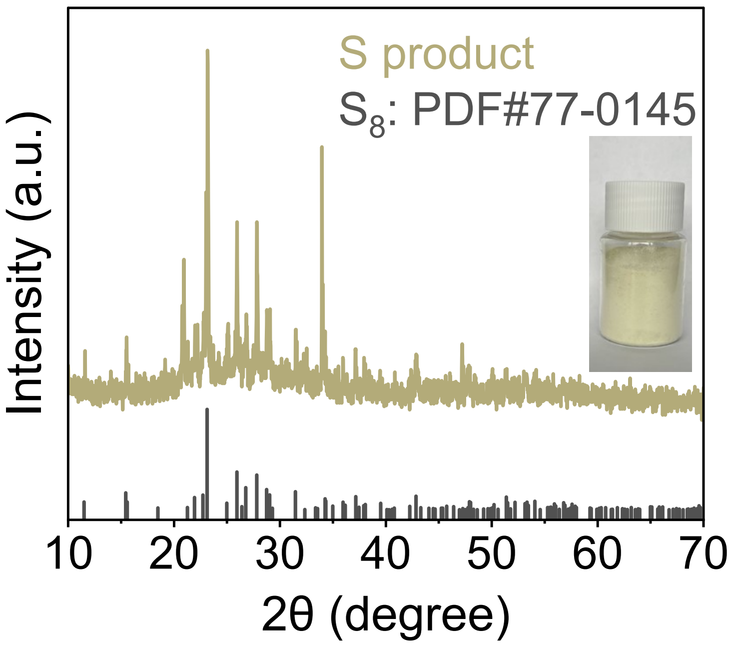

Fig. S13 XRD pattern of the collected S product.Inset: Digital image of S product.

Table S1 The comparison of HER performance of $Ni_2P/NiCr(OH)_2$ with reported catalysts.

Catalysts	Voltage at 10 mA cm^{-2} (V)	Voltage at 300 mA cm^{-2} (V)	Electrolytes	Reference electrode	Reference
$Ni_2P/NiCr(OH)_2$	0.110	0.277	1 M KOH	Hg/HgO	This work
NiFeP/SG	0.115	—	1 M KOH	Ag/AgCl	S1
NiFe-MoF	0.116	~0.250	1 M KOH	Hg/HgO	S2
CeO_2-LDH/Ni_3S_2/MoS_2	0.116	~0.280	1 M KOH	Ag/AgCl	S3
Co-Fe_2P	0.117	~0.260	1 M KOH	Hg/HgO	S4
Mo@$NiSe_2$	0.118	—	0.5 M H_2SO_4	Ag/AgCl	S5
CoNiFe/MnO@CNTs	0.122	—	1 M KOH	Ag/AgCl	S6
$Fe_2(MoO_4)_3$@GQD-NF-1	0.136	~0.270	1 M KOH	Hg/HgO	S7
WSe_2-CuO	0.141	—	0.5 M H_2SO_4	Ag/AgCl	S8
Co_9S_8@Co_9S_8@MoS_2-0.5	0.173	—	1 M KOH	Ag/AgCl	S9
NiMo-MOF	0.192	—	1 M KOH	Ag/AgCl	S10
$NiFe_2O_4$/NiO/g-C_3N_4	0.206	—	1 M KOH	——	S11
ReS_2/CoS@NF	0.213	—	1 M KOH	Ag/AgCl	S12
EM-FeNiP@HCNT	0.224	—	0.1 M KOH	Ag/AgCl	S13
CSMX-800	0.270	—	1 M KOH	Hg/HgO	S14
Ti_3C_2-CoS_2	0.276	—	1 M KOH	Ag/AgCl	S15

Table S2 The comparison of SOR performance of $Ni_2P/NiCr(OH)_2$ with reported catalysts.

Catalysts	Voltage at 100 mA cm^{-2} (V)	Voltage at 300 mA cm^{-2} (V)	Electrolytes	Reference electrode	Reference
$Ni_2P/NiCr(OH)_2$	0.363	0.401	1 M NaOH+1 M Na_2S	Hg/HgO	This work
Co_xP/NF	0.386	~0.580	1 M KOH+1 M Na_2S	Hg/HgO	S16
Co_9S_8/CoOOH	0.417	~0.610	1 M NaOH+1 M Na_2S	Hg/HgO	S17
IrO_2	0.430	—	1 M NaOH+1 M Na_2S	Hg/HgO	S18
NiFe-LDH/$FeNi_2S_4$/NF	0.440	—	1 M KOH+1 M Na_2S	Hg/HgO	S19
CoNiS	0.456	~0.600	1 M NaOH+1 M Na_2S	Hg/HgO	S20
Pdene@Om	0.458	—	1 M KOH + 3 M Na_2S	Hg/HgO	S21
TPA@Ni_3S_2	0.480	~0.600	1 M NaOH+1 M Na_2S	Hg/HgO	S22
np-NiMo-S	0.486	—	1 mol/L KOH + 1 mol/L Na_2S + seawater	Hg/HgO	S23
CuS/Ru-30	0.490	—	1 M NaOH+1 M Na_2S	Hg/HgO	S24
NiSe/NF	0.500	~0.640	1 M NaOH+1 M Na_2S	Hg/HgO	S25
Au@MoS_2	0.520	—	1 M KOH+ 0.5 M Na_2S	Ag/AgCl	S26
CoS/MoS_2	0.590	—	1 M NaOH+1 M Na_2S	Hg/HgO	S27
Ru-Ni_3S_2/NF	0.598	—	1.0 M NaOH +1.75 M Na_2S	Hg/HgO	S28
CoNiOOH	0.650	—	1 M KOH+ 0.5 M Na_2S	Ag/AgCl	S29

Table S3 The comparison of HWE performance of $Ni_2P/NiCr(OH)_2$ with reported catalysts.

Catalysts	Voltage at 100 mA cm^{-2} (V)	Voltage at 300 mA cm^{-2} (V)	Electrolytes	Reference
$Ni_2P/NiCr(OH)_2$	0.697	0.830	HER(1 M KOH)+SOR(1 M NaOH+1 M Na_2S)	This work
Ag-Ni_3S_2/NF	0.749	—	HER(1 M KOH)+SOR(1 M NaOH+2 M Na_2S)	S30
RuO_2-Co_3O_{4-X}	0.750	~1.600	HER(1 M NaOH+0.5 M NaCl)+SOR(1 M NaOH+1 M Na_2S)	S31
$CoS_2/MoS_2/CoMoO_4$/NF	0.770	—	HER(1 M NaOH+0.5 M NaCl)+SOR(1 M NaOH+1 M Na_2S)	S32
V_{Pd}-Pd_4S_{MNRs}	0.776	~1.000	HER(1 M NaOH in sweater)+SOR(1 M NaOH+1 M Na_2S)	S33
S-$NiMoO_4$/NF	0.800	—	HER(1 M KOH)+SOR(1 M KOH+1 M Na_2S)	S34
Ni_3P NS@NC/NF	0.806	~1.000	HER(1 M NaOH)+SOR(1 M KOH+1 M Na_2S)	S35
$FeSe_2$/IF-V_{Se}	0.900	—	HER(1 M NaOH)+SOR(1 M NaOH+1 M Na_2S)	S36

References

[S1] R. Li, B. Wang, T. Gao, R. Zhang, C. Xu, X. Jiang, J. Zeng, Y. Bando, P. Hu, Y. Li and X. Wang, *Nano Energy*, 2019, **58**, 870.

[S2] B Dai, X Wei, L Chen, X Bao, Q Zhong, H Qu, *J. Colloid Interface Sci.*, 2025, **682**, 80-93.

[S3] H. Li, F. Chen, X. Wu, D. Wang, Y. Ren, Y. Li, *Materials*, 2024, **17**, 4876.

[S4] S. Wang, P. Yang, X. Sun, H. Xing, J. Hu, P. Chen, Z. Cui, W. Zhu and Z. Ma, *Appl. Catal., B*, 2021, **297**, 120386.

[S5] M. Pratheeksha, N. Hemavathi, D. Sumanth, S.Kalyan, B.Geetha, R. Shwetharani, *Energy Fuels*, 2025, **39**, 6930-6941.

[S6] C. Zhou, X. Han, F. Zhu, X. Zhang, Y. Lu, J. Lang, X. Cao, H Gu, *Int. J. Hydrogen Energy*, 2022, **47**, 27775-27786.

[S7] Z. Yin, B. Zhang, Q. Zhang, Y. Zhou, J. Li, Y. Wang, L. Wan, Z. Ma, *J. Mol. Struct.*, 2025, **1329**, 141402.

[S8] R. Patel, P. Pataniya, S. Siraj, P. Sahatiya, C. Sumesh, *Renewable Energy*,2024, **55**, 815-827.

[S9] J. Li, G. Li, J. Wang, C. Xue, X. Li, S. Wang, B. Han, M. Yang, L. Li, *Inorg. Chem. Front.*, 2020, **7**, 191-197.

[S10] R. Pavadai, M. Arivazhagan, S. Prabu, S. Ingavale, G. Honnu, V. Gowri, S. Thongmee, C. Issro, D. Khamboonrueang, S. Kityakarn, *Mater. Chem. Phys.*, 2025, **345**, 131245.

[S11] M. Begam, L. Kumaresan, S. Hemapriya, P. Velusamyc, S. Ashokd, N. Dineshbabu, *Diamond Relat. Mater.*, 2025, **157**, 112489.

[S12] N. Trivedi, P. Sharma, K. Joshi, V. Patel, CK. Sumesh, P. Pataniya, *Int. J. Hydrogen Energy*, 2024, **61**, 1212-1219.

[S13] M. Zheng, K. Shi, Y. Zhao, T. Zhang, F. Liu, J. Liu, Y. Sun, Y. Zhang, H. Wang, *Int. J. Hydrogen Energy*, 2024, **72**, 1077-1090.

[S14] K. Farooq, M. Murtaza, Z. Yang, A. Waseem, Y. Zhu, Y. Xia, *Nanoscale Adv.*, 2024, **6**, 3169-3180.

[S15] S. Devi, R. Navamathavan, *J. Electrochem. Soc.*, 2023, **170**, 096503.

[S16] H. Chen, M. Xiong, S. Qiao, S. Wu, C. Rao, G. Luo, L. Wang, S. Ci, Z. Wen, *Chem. Eng. J.*, 2025, **524**, 169400.

[S17] Y. Pan, P. Dai, Z. Yang, X. Tang, K. Wang, M. Wu, *Dalton Trans.*, 2025, **54**, 10589-10598.

[S18] M. Zhang, J. Guan, Y. Tu, S. Chen, Y. Wang, S. Wang, L. Yu, C. Ma, D. Deng and X. Bao, *Energy Environ. Sci.*, 2020, **13**, 119.

[S19] L. Ai, Y. Tian, T. Xiao, J. Zhang, C. Zhang, J. Jiang, *J. Colloid Interface Sci.*, 2024, **673**, 607-615.

[S20] D. Wu, W. Wang, J. Li, H. Dong, H. Shi, J. Qin, Y. Hu, L. Cao, B. Dong, *Int. J. Hydrogen Energy*, 2026, **201**, 153013.

[S21] H. Sun, C. Wangzi, Z. Yang, J. Zhang, Y. Liang, J. Wang, Y. Zheng, J. Pan, C. Li, J. Cao, *Appl. Catal., B*, 2026, **381**, 125888.

[S220] L. Jin, C. Chen, L. Hu, X. Liu, Y. Ding, J. He, H. Li, N. Li, D. Chen, Q. Xu, J. Lu, *Appl. Surf. Sci.*, 2022, **605**, 154756.

[S23] M. Yang, J. Ding, Z. Wang, J. Zhang, Z. Peng, X. Liu, *Chin. Chem. Lett.*, 2025, **36**, 110861.

[S24] A. Min, V. Maheskumar, D. Lee, A. Kumar, M. Joo, S. Arumugam, C. Yong, *J. Energy Chem.*, 2024, **99**, 541-552.

[S25] C. Duan, C. Tang, S. Yu, L. Li, J. Li, Y. Zhou, *Appl. Catal., B*, 2023, **324**, 122255.

[S26] M. Shi, H. Yang, X. Xiao, P. Jin, Y. Chen, *Chem. Eng. J.*, 2025, **522**, 167474.

[S27] K. Gao, M. Zhou, Y. Liu, S. Wang, R. Fu, Z. Wang, J. Guo, Z. Liu, H. Wang, Y. Zhao, Q. Wang, *J. Colloid Interface Sci.*, 2024, **657**, 290-299.

[S28] Q. Zeng, L. Ai, X. Liu, A. Liu, J. Jiang, *Chem. Eng. J.*, 2025, **524**, 169473.

[S29] M. Yang, T. Wei, C. Zeng, J. Zhang, Y. Liu, J. Luo, G. Hu, X. Liu, *Chem. Eng. J.*, 2024, **498**, 155799.

[S30] M. Ming, J. Kang, Y. Gu, J. Zhang, Q. Zhang, G. Fan, Q. Shen, *J. Environ. Chem. Eng.*, 2025, **13**, 119139.

[S31] H. Yang, X. Long, F. Liu, J. Zhou, N. Chen, R. Feng, Y. Zhang, X. Fu, J. Luo, B. Zhao, *Appl. Catal., B*, 2025, **366**, 125037.

[S32] K. Tang, C. Yang, S. Zhang, J. Yang, L. Shi, S. Xiong, A .Tang, *Int. J. Hydrogen Energy*, 2025, **163**, 150823.

[S33] W. Wang, Q. Mao, S. Jiang, K. Deng, H. Yu, Z. Wang, Y. Xu, L. Wang, H. Wang, *Appl. Catal., B*, 2024, **340**, 123194.

[S34] Y. Chen, Y. Wang, B. Liu, C. Zhang, D. Sun, H. Liu, W. Zhou, *J. Colloid Interface Sci.*, 2024, **664**, 469-477.

[S35] K. Tong, W. Qiu, S. Zhang, W. Zhao, P. Wu, F. Lin, L. Chu, H. Wang, W. Tian, M. Huang, *Chem. Eng. J.*, 2025, **510**, 161611.

[S36] X. Wang, J. Jiang, J. Zhang, Q. Zeng, A. Liu, L. Ai, *J. Colloid Interface Sci.*, 2025, **684**, 367-376.